DNA binding properties, histidine interaction and cytotoxicity studies of water soluble ruthenium(II) terpyridine complexes.

Dejan Lazića,[a] Aleksandar Arsenijević,[a] Ralph Puchta,[c,d] Živadin D. Bugarčić[b] and Ana Rilak*[b]

[a] *Faculty of Medicine, Centre for Molecular Medicine and Stem Cell Research, University of Kragujevac, Svetozara Markovića 69, 34000 Kragujevac, Serbia*

[b] *Department of Chemistry, Faculty of Science, University of Kragujevac, Radoja Domanovića 12, P. O. Box 60, 34000 Kragujevac, Serbia*

[c] *Institute for Inorganic Chemistry, Department of Chemistry and Pharmacy, University of Erlangen-Nürnberg, Egerlandstraße 1, 91058 Erlangen, Germany.*

[d] *Computer Chemistry Center, Department of Chemistry and Pharmacy, University of Erlangen-Nürnberg, Nägelsbachstraße 25, 91052 Erlangen, Germany*

**Corresponding author:* Dr. Ana Rilak
Department of Chemistry,
Faculty of Science,
University of Kragujevac,
Radoja Domanovića 12
Tel: +381(0)34300262
Fax: +381(0)34335040
e-mail: anarilak@kg.ac.rs

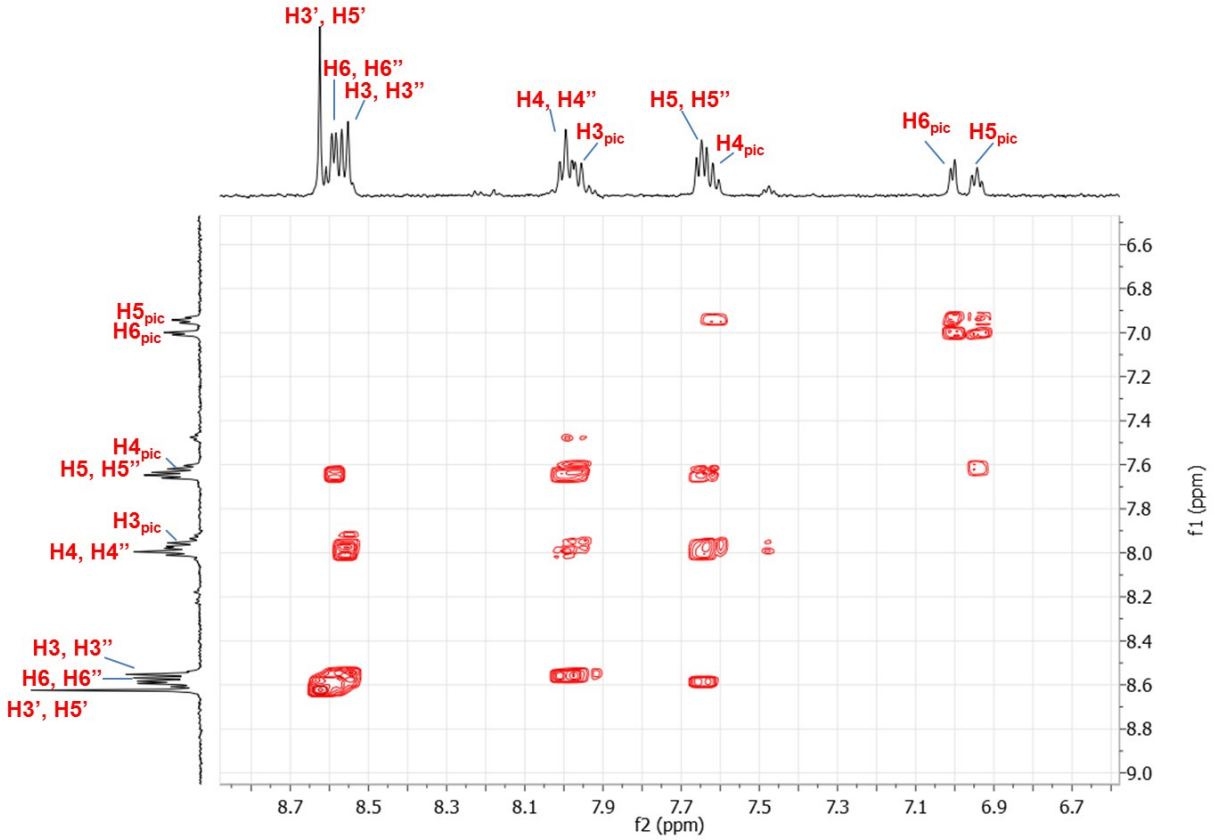

Fig. S1. ^{1}H-^{1}H COSY NMR spectrum of complex **4** in a mixture of acetone-d^{6}/D_2O (6 : 1) at 298 K.

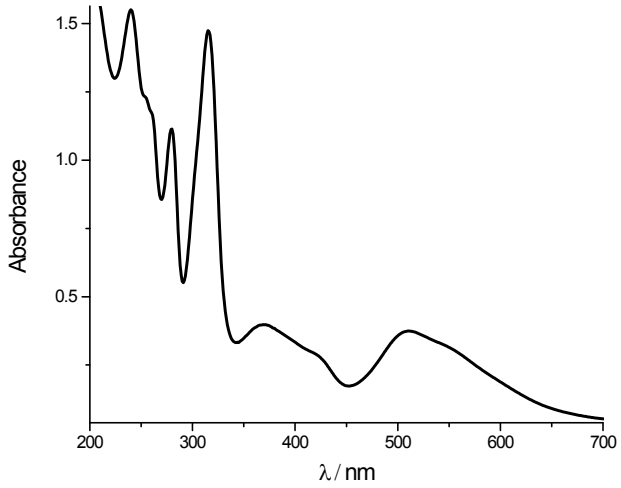

Fig. S2. UV-Vis spectrum of complex **4** (3 x 10^{-5}M) in acetonitrile.

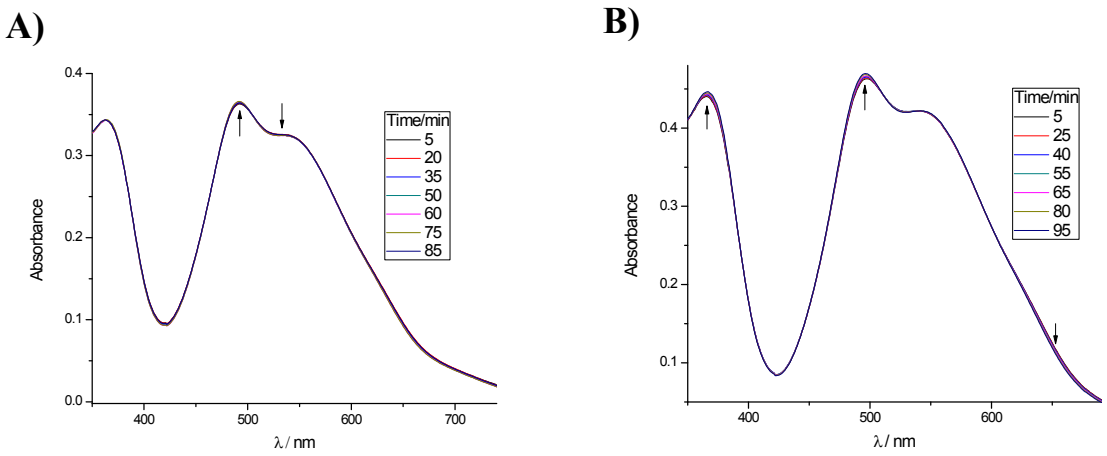

Fig. S3. Time evolution of UV-Vis spectra during the interaction of the complexes A) [Ru(Cl-tpy)(en)Cl][Cl] (**1**) and B) [Ru(Cl-tpy)(dach)Cl][Cl] (**2**) with L-His in 25 mM Hepes buffer containing 30 mM NaCl (pH 7.4) at 310 K.

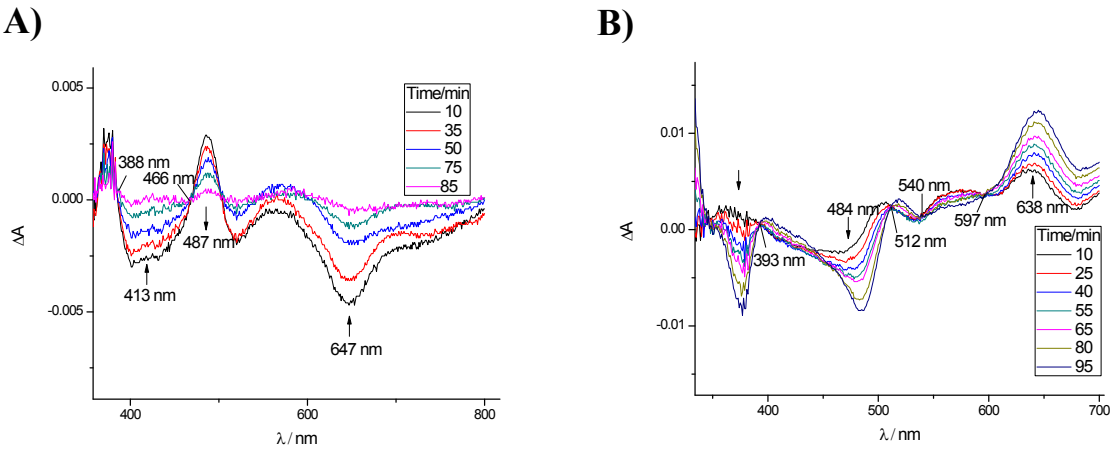

Fig. S4. Time evolution of UV-Vis difference spectra during the interaction of the complexes A) [Ru(Cl-tpy)(en)Cl][Cl] (**1**) and B) [Ru(Cl-tpy)(dach)Cl][Cl] (**2**) with L-His in 25 mM Hepes buffer containing 30 mM NaCl (pH 7.4) at 310 K. $\Delta A = A_t - A_0$, where A_t = absorbance at time t and A_0 = absorbance at the time at which the first spectrum was recorded.

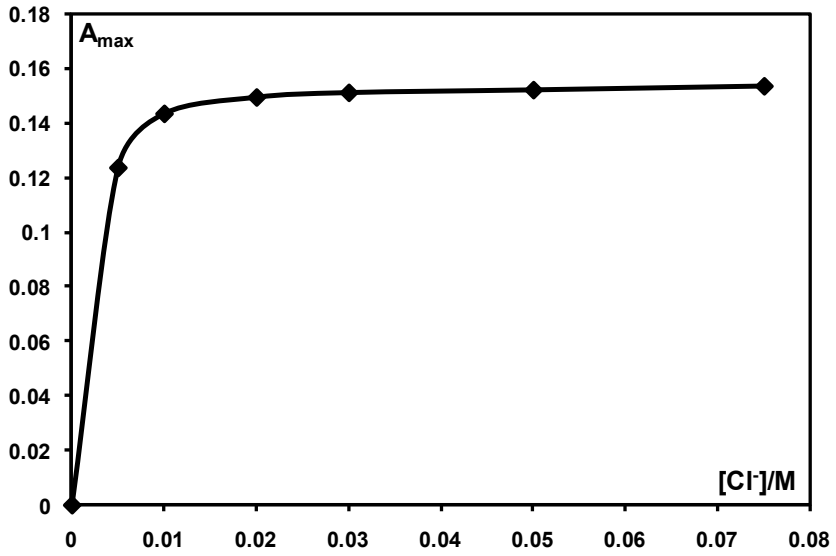

Fig. S5. The change of absorbance at 401 nm of the $[Ru(Cl\text{-}tpy)(en)Cl]^+$ (**1**) complex *vs*. $[Cl^-]$ in 0.1M $NaClO_4$ at 310 K.

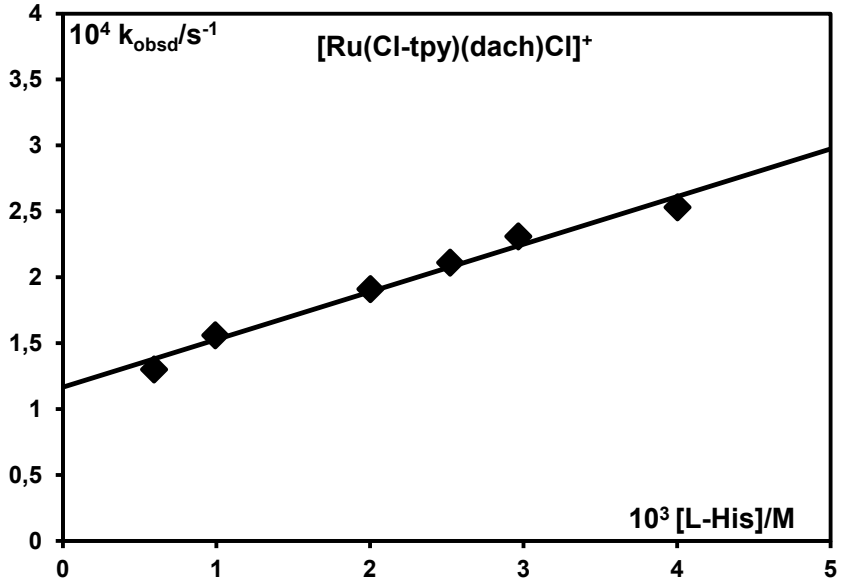

Fig. S6. *Pseudo* first-order rate constants, k_{obsd}, plotted as a function of ligand concentration for the substitution reaction of $[Ru(Cl\text{-}tpy)(dach)Cl]^+$ (**2**) with L-His in 25 mM Hepes buffer (30 mM NaCl, pH 7.4).

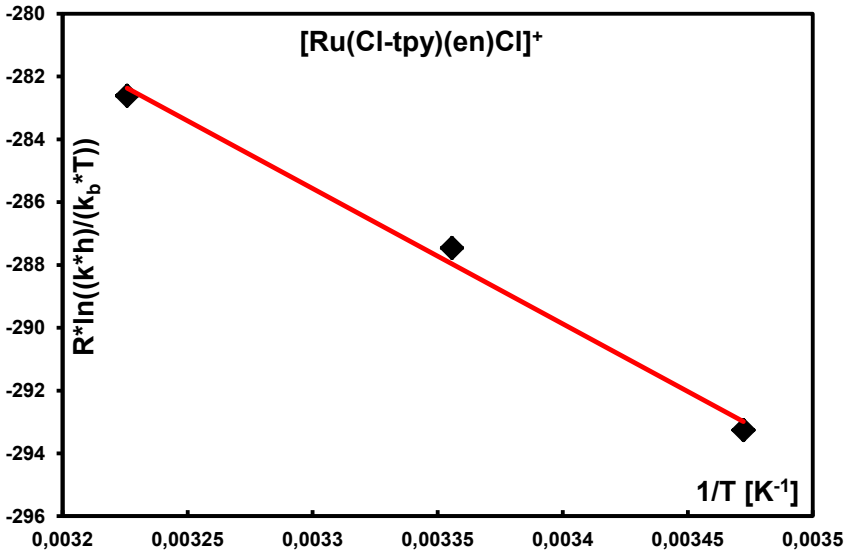

Fig. S7. Eyring plot for the reactions of complex **1** with L-His, at pH 7.40 in 25 mM Hepes buffer and 30 mM NaCl.

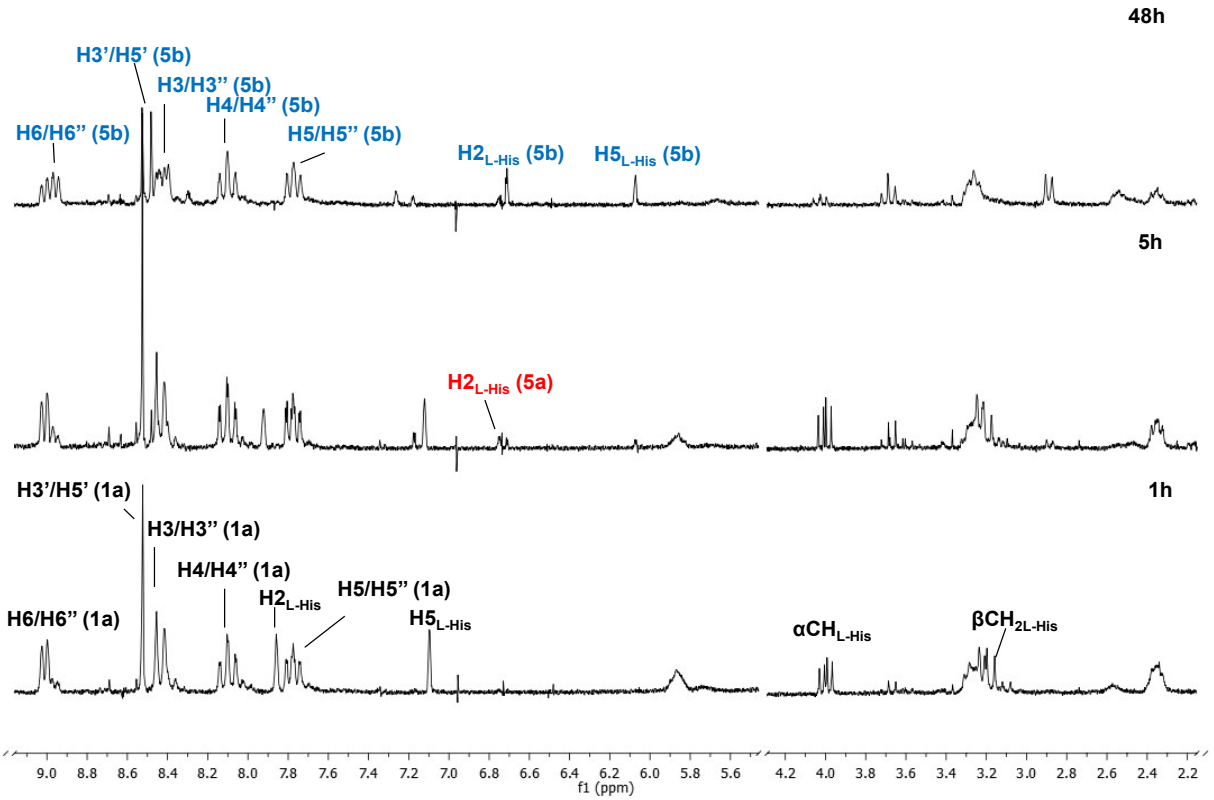

Fig. S8. ^{1}H NMR spectra of $[Ru(Cl\text{-}tpy)(en)H_2O)]^{2+}$ (**1a**, 10 mM) at various time intervals after addition of L-His (1 eq, pH = 5.35, 295 K).

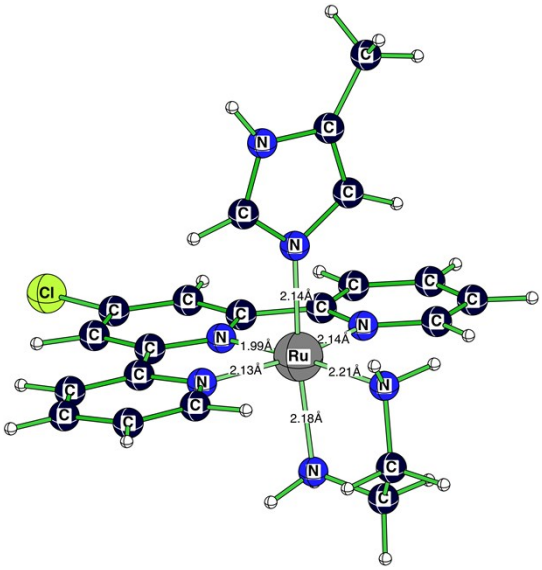

0.0 kcal/mol (0.0 kcal/mol)

[Ru(Cl-tpy)(en)(4-methylimidazole-*N1*)]$^{2+}$

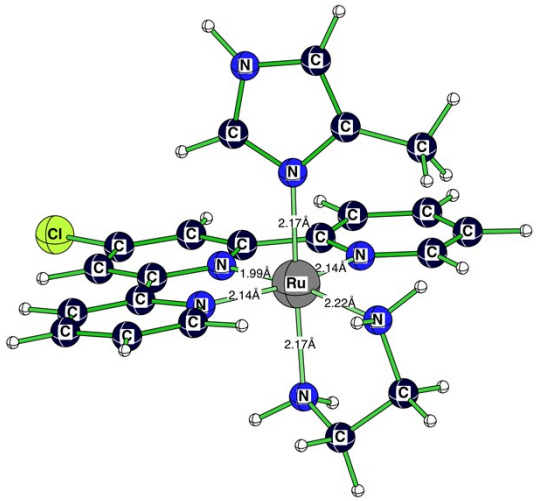

5.4 kcal/mol (4.5 kcal/mol)

[Ru(Cl-tpy)(en)(4-methylimidazole-*N3*)]$^{2+}$

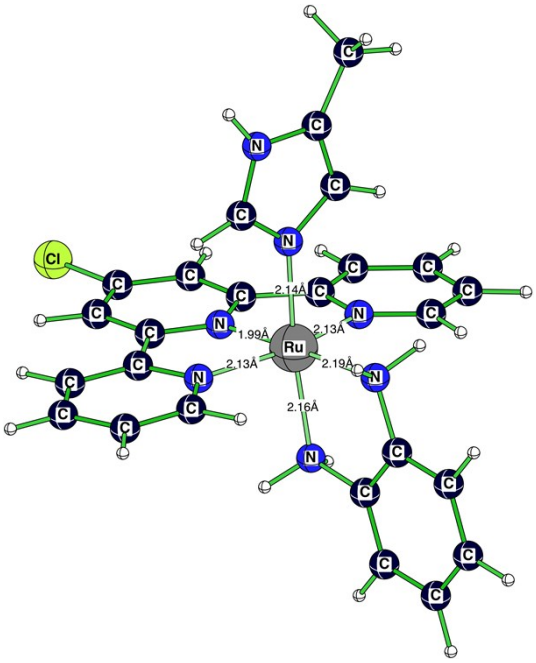

0.0 kcal/mol (0.0 kcal/mol)

[Ru(Cl-tpy)(dach)(4-methylimidazole-*N1*)]$^{2+}$

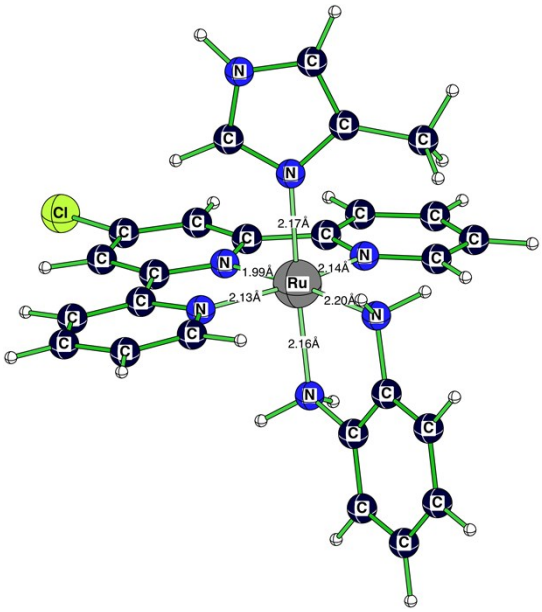

5.4 kcal/mol (4.3 kcal/mol)

[Ru(Cl-tpy)(dach)(4-methylimidazole-*N3*)]$^{2+}$

Fig. S9. Calculated (B3LYP/LANL2DZp) isomeric structures and energies (B3LYP/LANL2DZp + ZPE((B3LYP/LANL2DZp)) of [Ru(Cl-tpy)(en)(4-

methylimidazole)]$^{2+}$ and [Ru(Cl-tpy)(dach)(4-methylimidazole)]$^{2+}$. Values in brackets: B3LYP(CPCM)/LANL2DZp//B3LYP/LANL2DZp + ZPE(B3LYP/LANL2DZp).

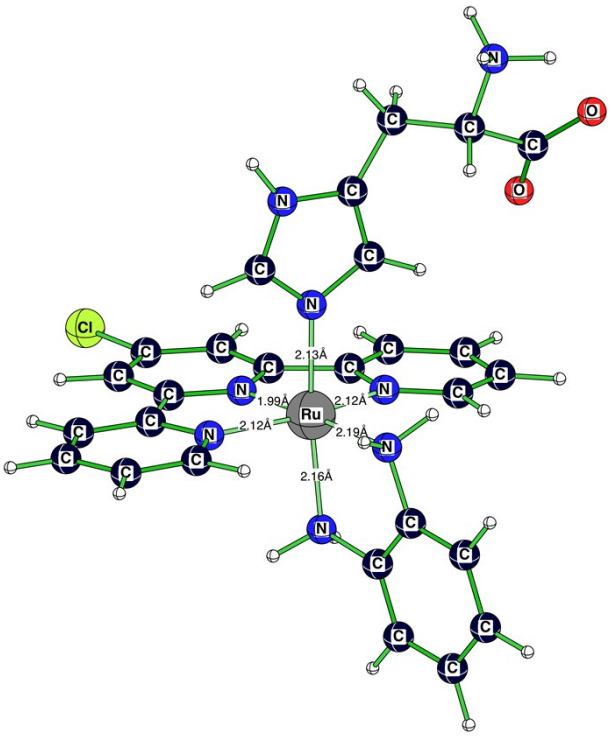

0.0 kcal/mol

N1- coordinated L-His in [Ru(Cl-tpy)(dach)(L-His)]$^{2+}$

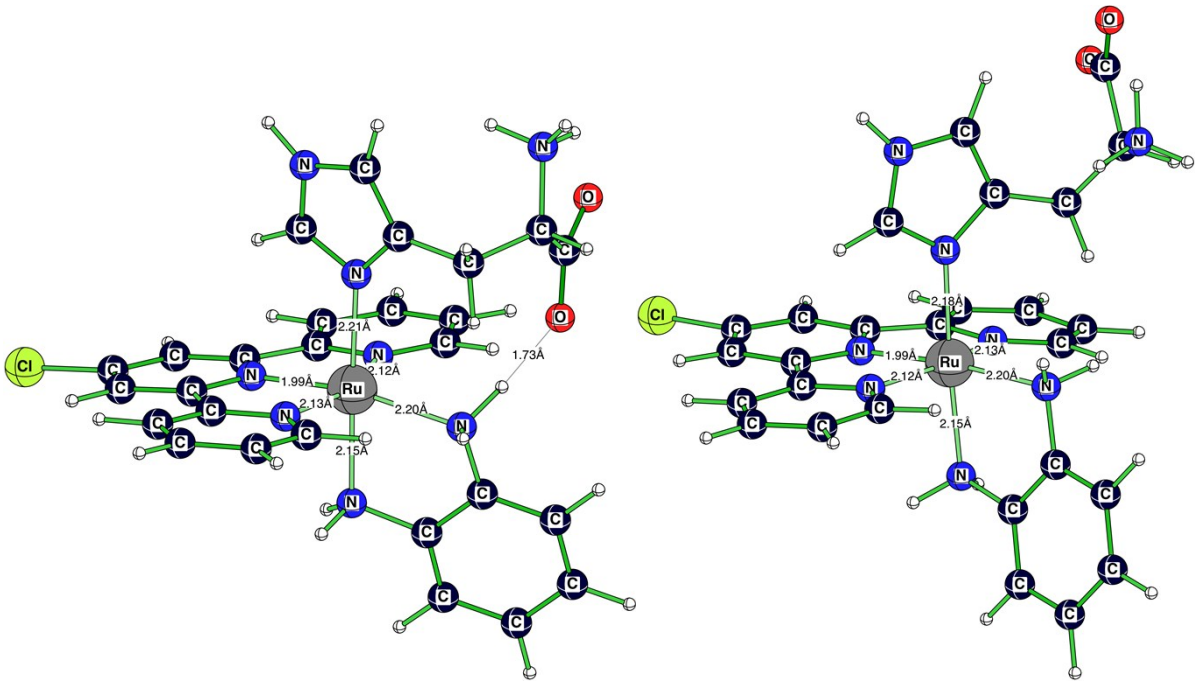

-1.0 kcal/mol 3.8 kcal/mol

N3- coordinated L-His in $[Ru(Cl\text{-}tpy)(dach)(L\text{-}His)]^{2+}$ with and without an inner molecular hydrogen bond

Fig. S10. Calculated (B3LYP(CPCM)/LANL2DZp) N1- and N3 bound isomeric structures and energies (B3LYP(CPCM)/LANL2DZp + ZPE(B3LYP(CPCM)/LANL2DZp)) of $[Ru(Cl\text{-}tpy)(dach)(L\text{-}His)]^{2+}$. In the case of the N3-coordinated species rotamers with and without an inner molecular hydrogen bond is considered.

DNA-binding studies

Calculation of DNA-binding constants

In order to compare quantitatively the binding strength of the complexes, the intrinsic binding constants K_b were determined by monitoring the changes in absorption at the MLCT band with increasing concentration of CT DNA using the following equation (1)[S1]

$$[DNA]/(\varepsilon_A - \varepsilon_f) = [DNA]/(\varepsilon_b - \varepsilon_f) + 1/[K_b(\varepsilon_b - \varepsilon_f)] \quad \text{(S1)}$$

K_b is given by the ratio of slope to the *y* intercept in plots $[DNA]/(\varepsilon_A - \varepsilon_f)$ *versus* [DNA] (Fig. S12), where [DNA] is the concentration of DNA in base pairs, $\varepsilon_A = A_{obsd}/[complex]$, ε_f is the extinction coefficient for the unbound complex and ε_b is the extinction coefficient for the complex in the fully bound form.

Stern-Volmer equation for EB competitive studies

The relative binding of complexes to CT-DNA was determined by calculating the quenching constant (K_{sv}) from the slopes of straight lines obtained from Stern-Volmer Eq. (2)[S2]:

$$I_0/I = 1 + K_{sv}[Q] \quad \text{(S2)}$$

where I_0 and I are the emission intensities in the absence and the presence of the quencher (complexes **1** and **2**), respectively, [Q] is the total concentration of quencher, K_{sv} is the Stern-Volmer quenching constant which can be obtained from the slope of the plot of I_0/I *versus* [Q] (Fig. 6).

References

S1. A. M. Pyle, J. P. Rehmann, R. Meshoyrer, C. V. Kumar, N. J. Turro and J. K. Barton, *J. Am. Chem. Soc*., 1989, **111**, 3051-3058.

S2. R. Lakowicz and G.Weber, *Biochemistry*, 1973, **12**, 4161-4170.

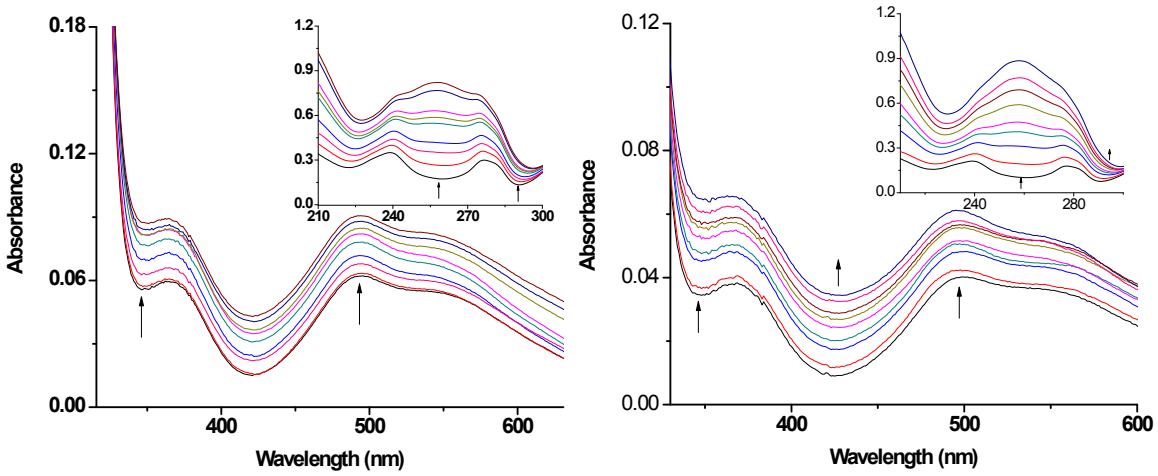

Fig. S11. Absorption spectra of the complexes **1** (left) and **2** (right) in Tris-HCl buffer upon addition of calf thymus DNA. [Ru] = 1.25 x 10^{-5} M, [DNA] = (0.12-1.25) x 10^{-4} M. Arrow shows the absorbance changing upon increasing DNA concentrations. Insets: spectral changes of **1** and **2** ranging between 200 and 300 nm.

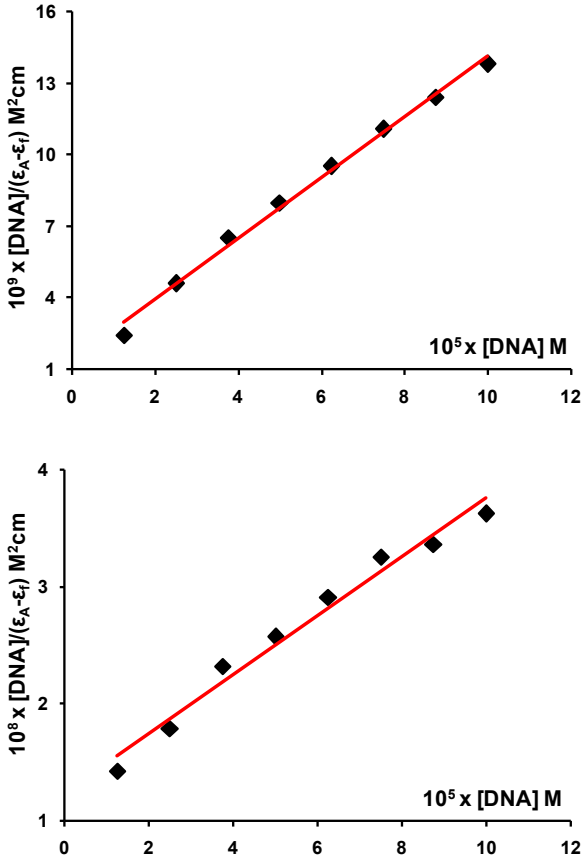

Fig. S12. Plots of [DNA]/($\varepsilon_A - \varepsilon_f$) *versus* [DNA] for the complexes **1** (top) and **2** (bottom).

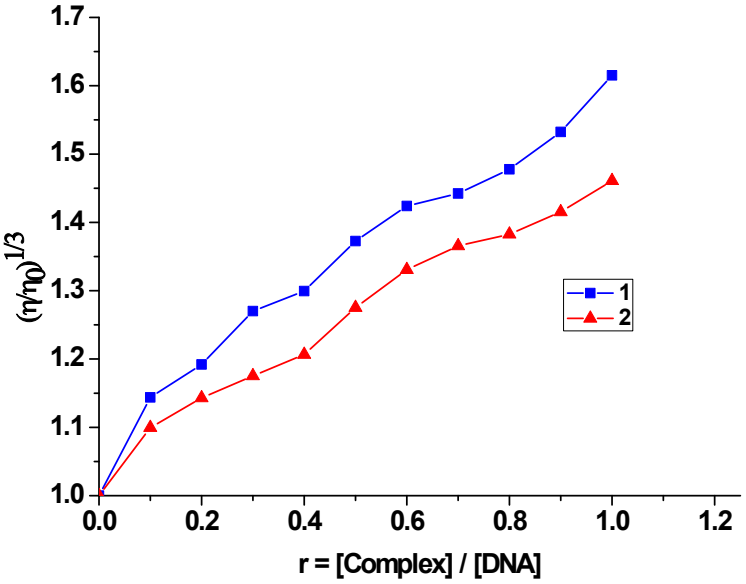

Fig. S13. Relative viskosity $(\eta/\eta_0)^{1/3}$ of CT DNA (0.01 mM) in buffer solution (150 mM NaCl and 10 mM Tris-HCl at pH 7.4) in the presence of the complexes **1** and **2** at increasing amounts (*r*).

Table S1. Observed *pseudo*-first order rate constants as a function of ligand concentration and temperature for the substitution reactions between [Ru(Cl-tpy)(en)Cl][Cl] (**1**) and L-His in 25 mM Hepes buffer containing 30 mM NaCl (pH=7.4).

λ/nm	**T/K**	**10^3 C_L/M**	**10^4 k_{obsd}/s^{-1}**
487	288	4.00	0.96(2)[a]
		3.00	0.90(3)
		2.52	0.50(3)
		2.20	0.42(2)
		1.00	0.32(2)
		0.60	0.30(3)
	298	4.00	1.90(2)
		3.00	1.80(2)
		2.52	1.71(2)
		2.20	1.52(3)
		1.00	0.90(3)
		0.60	0.70(3)
	310	4.00	3.80(2)
		3.00	3.10(2)
		2.52	2.80(2)
		2.20	2.51(3)
		1.00	1.90(3)
		0.60	1.30(3)

[a] Number of runs in parenthesis

Table S2. Observed *pseudo*-first order rate constants as a function of ligand concentration for the substitution reactions between [Ru(Cl-tpy)(dach)Cl][Cl] (**2**) and L-His in 25 mM Hepes buffer containing 30 mM NaCl (pH=7.4).

λ(nm)	**T(K)**	**10^3 C_L/M**	**10^4 k_{obsd}/s^{-1}**
638	310	4.00	2.53(2)[a]
		3.00	2.31(2)
		2.52	2.11(3)
		2.20	1.91(3)
		1.00	1.56(3)
		0.60	1.30(3)

[a] Number of runs in parenthesis

Table S3. Selected chemical shifts for the investigated ligands and the products from their reactions with **1** and **2**.

Species	***δ* (H6/H6")**	***δ* ($H2_{L\text{-}His}$)**	***δ* ($H5_{L\text{-}His}$)**
1a	9.01		
2a	9.06/8.96		
L-His		8.01	7.15
5a	n.a.	6.75	n.a.
5b	8.95	6.71	6.07
L-His		7.86	7.09
6a	n.a.	6.74	n.a.
6b	9.04/8.89	6.70	6.07

n.a. = not assigned